Supplementary Material

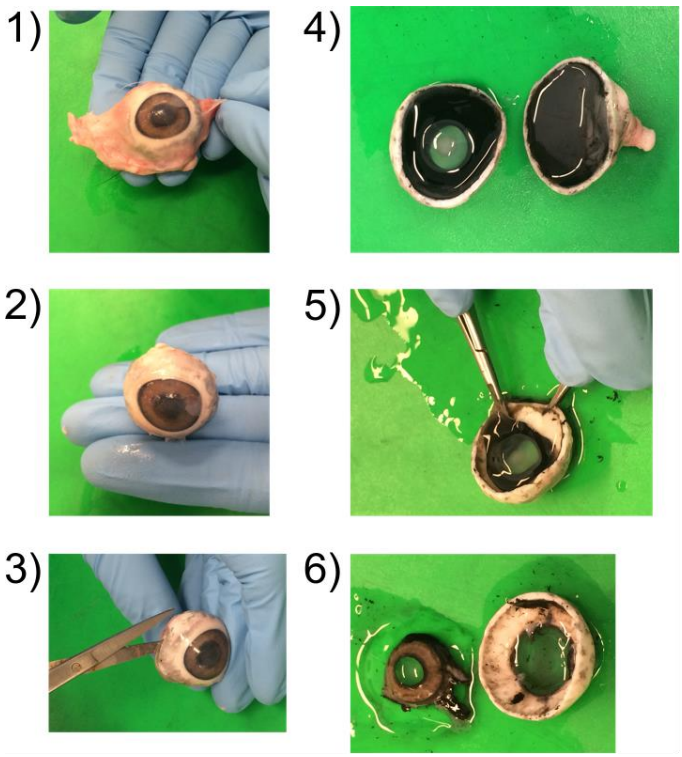

Figure S1 Caption: Careful dissections of eye globes were required to isolate the corneal endothelium with minimal damage during the dissection procedure. 1) Porcine eyes were obtained fresh from a local slaughterhouse. 2) Using gross dissection scissors, all extraocular muscles and orbital fat were first removed from the eye and using a #21 scalpel blade, the epithelium was gently scrapped off the cornear. 3) A #11 scalpel blade was used to puncture the scelera, and using a pair of gross dissection scissors and/or the #21 scalpel blade, the globe was cut along the equator of the sclera to 4) isolate the anterior portion of the eye. 5) The most difficult part of the dissection was separating the ciliary body and iris without damaging the underlying endothelium. Using a pair of serrated forceps, the sclera was held in place and the ciliary body and iris were detached from the sclera using Castroviejo scissors. The Castroviejo scissors were wedged in between the ciliary body and iris and were continuously rotated along the circumference of the anterior segment of the eye in a spiral-like manner carefully, until 6) the

ciliary body, lens, and remaining vitreous humor were able to be easily peeled off to expose the corneal endothelium.

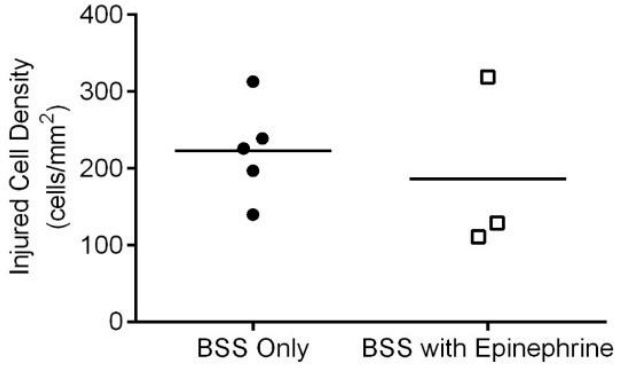

Figure S2 Caption: Injured/dead CEC densities over the full contact area in to the 9 mN indentation group. Three specimens were tested using previously opened BSS containers supplemented with 500 units of epinephrine from the Flaum Eye Institute operating room at the University of Rochester Medical Center after cataract surgery. Results fell within the range of injured/dead CEC densities of specimens tested with new (unopened) BSS.

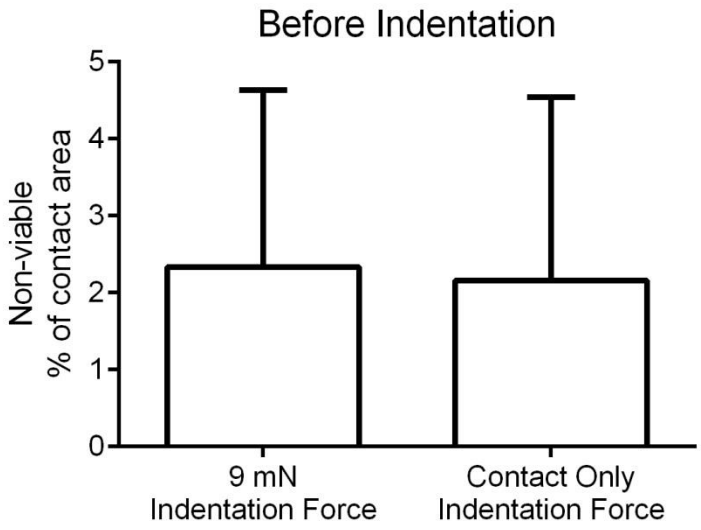

Figure S3 Caption: Calcein-negative areas (dark regions) within the contact area of all specimens in the 0.65 mN and 9 mN experimental groups prior to indentation were calculated via thresholding tools in ImageJ and MATLAB. The range of pixel intensities was found within

the contact area, and a threshold was applied to all pixels below 10-20 % of the range of pixel values, highlighting the dark regions only. To obtain the percentage of non-viable CECs in the contact area the total number of highlighted pixels after thresholding were divided by the total number of pixels in the contact area. Results expressed as mean + SD, p-value (> 0.05) after non-paired t-test.

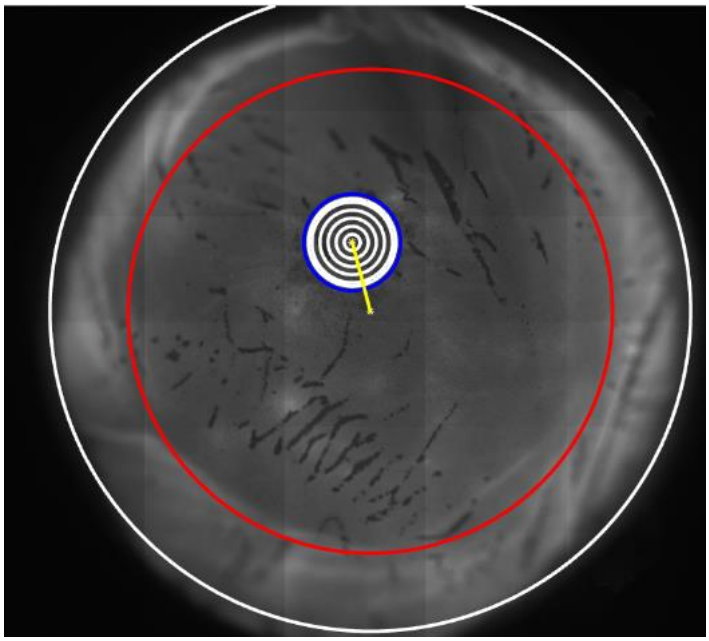

Figure S4 Caption: One elimination criteria was that indentation sites near the periphery were discarded. A circle-drawing function in MATLAB(Chernov, 2009) was utilized to draw the circumference of the specimen (white circle), and find the center of the specimen (white asterisk). The distance between the center of the indentation site (white bullseye) and the center of the specimen was calculated (yellow line). Only specimens with indentation sites less than 2 mm from the center of the specimen (within the red circle) were considered for analysis.

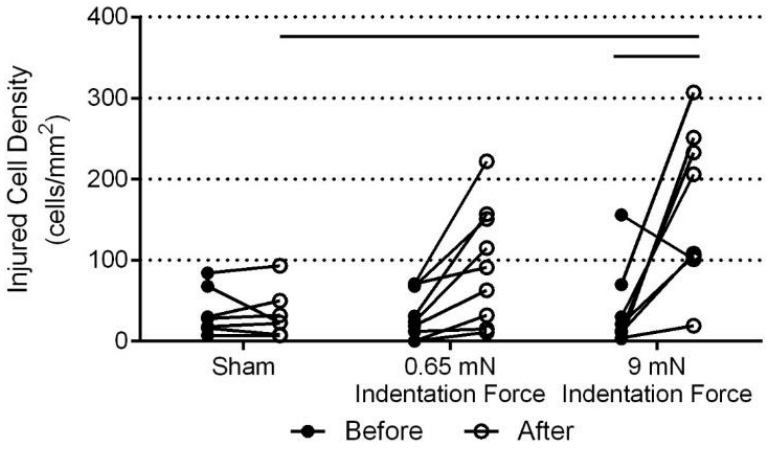

Figure S5 Caption: Quantification of injured CEC densities within the full contact area (same as Figure 6), but shown as a paired before-after plot. One specimen from the sham negative control group and one specimen from the 9 mN indentation group measured a decrease in injured cell density as compared to its baseline. All other specimens saw no, marginal, or substantial increases in injured dead/cell CEC densities after mechanical loading. This behavior could be explained by CECs getting stripped off the Descemet's membrane during the course of an experiment.

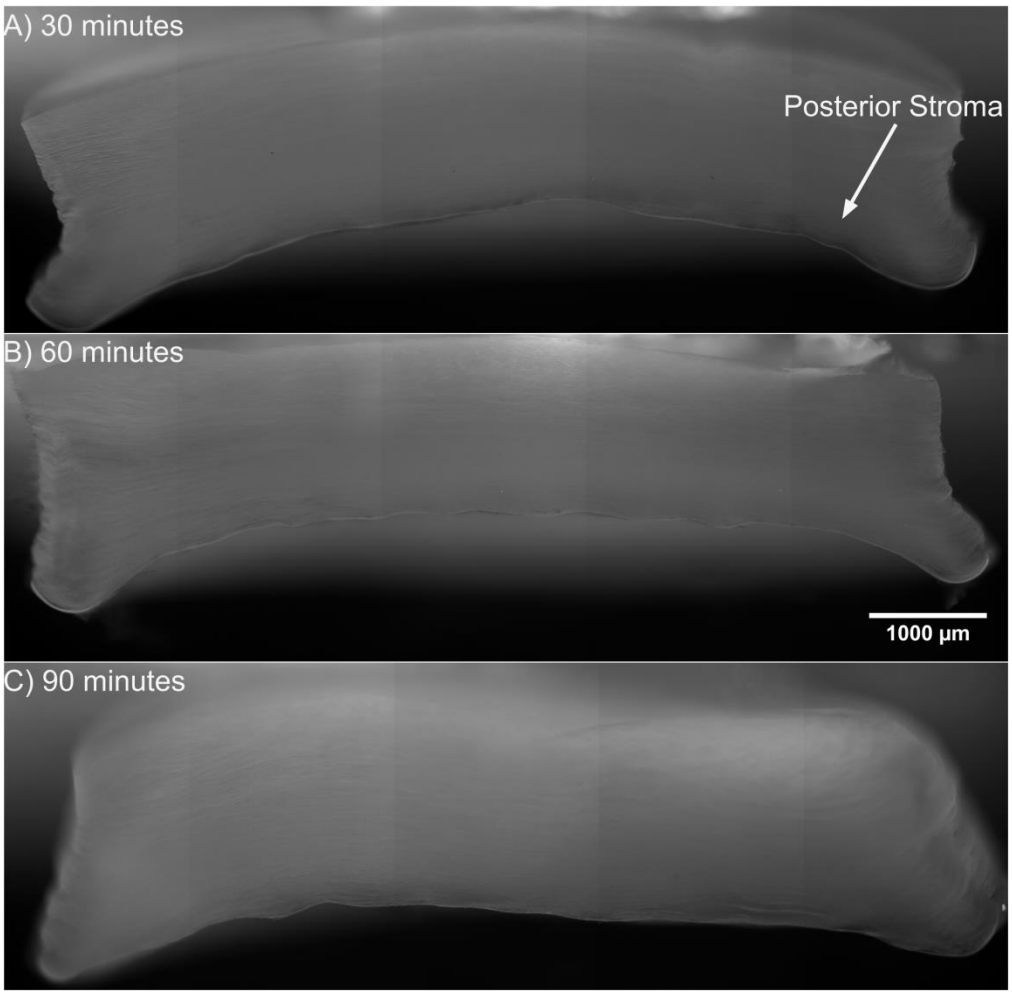

Figure S6 Caption: Cross-sectional images of representative 8 mm diameter corneal buttons fixed overnight in 4% PFA and bisected into hemi-cylinders after being allowed to swell for 30, 60, and 90 minutes. In all panels the posterior stroma is the bottom boundary. The posterior stroma swelled more than the anterior. Swelling-induced curvature appeared to concentrate in the peripheral edges of the button (i.e., not the center).

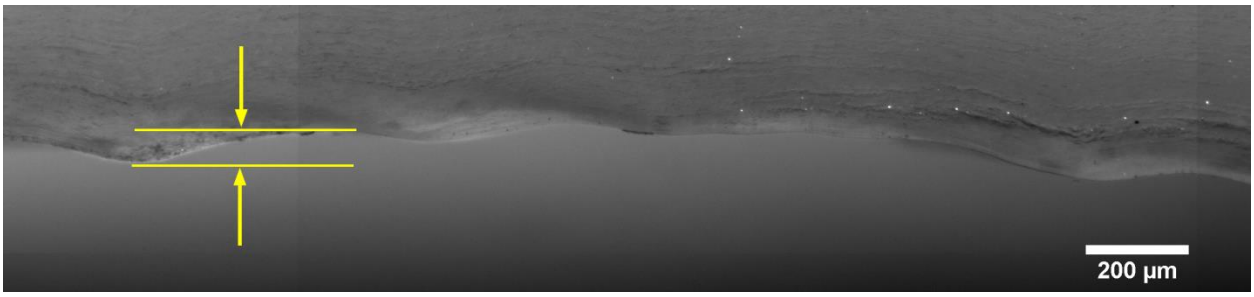

Figure S7 Caption: Zoomed in image of endothelial surface of a representative bisected hemi cylindrical button. The upper and lower surfaces between undulations were delineated in ImageJ. The distance between them was measured as the asperity (gap) height. While surface undulations were observed in all specimens, asperity height was not significant.

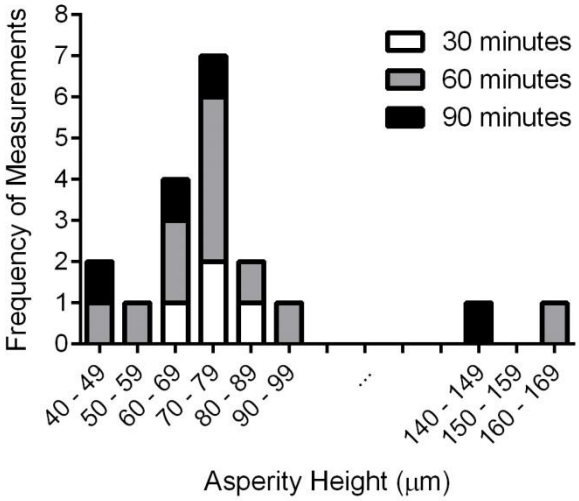

Figure S8 Caption: Histogram of asperity height measurements for all specimens (see Figures S6 and S7).

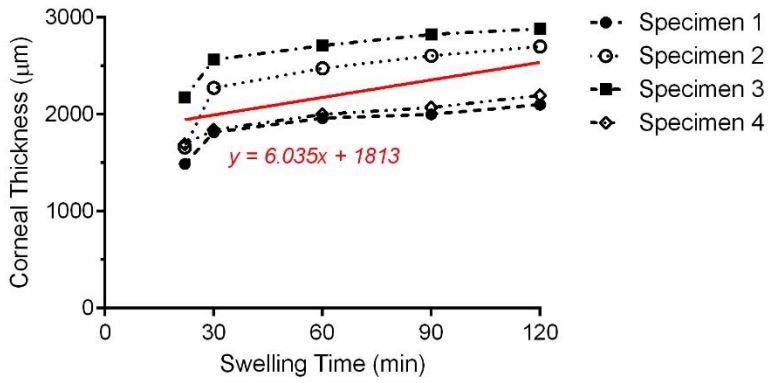

Figure S9 Caption: Corneal buttons were dissected as described in the manuscript and initially incubated for 35 minutes (equivalent length of time corneas remained immersed for staining) after which 8 mm diameter buttons were trephined. They were then allowed to swell over an additional 2 hours and changes in corneal thickness were measured. This simulated the waiting intervals corneoscleral rims underwent prior to testing in the manuscript. A linear regression was used to establish a relationship between corneal thickness and swelling time.

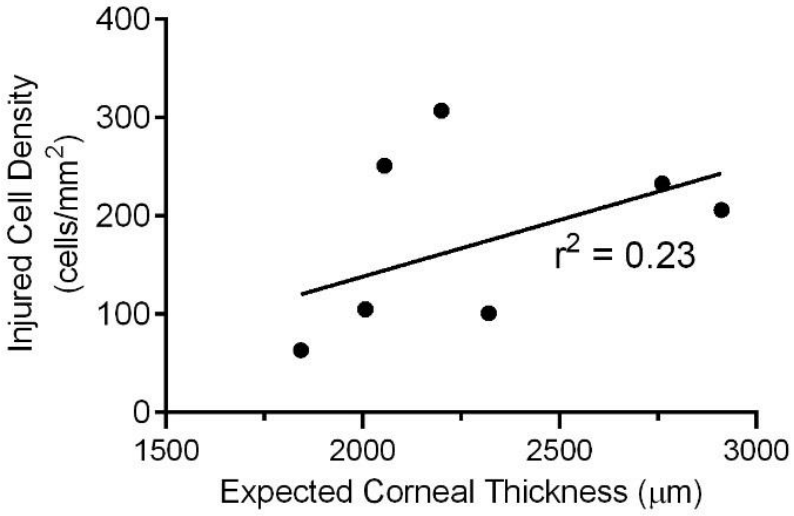

Figure S10 Caption: Injured/dead CEC densities for corneas in the 9 mN indentation force group expressed as a function of expected corneal button thickness. Corneal thickness was interpolated based on previous linear relationship (see Figure S9). The correlation between

increased CEC loss and corneal thickness is poor (r^2 = 0.23). Hence, the effects of swelling are weak compared to specimen-to-specimen variability.

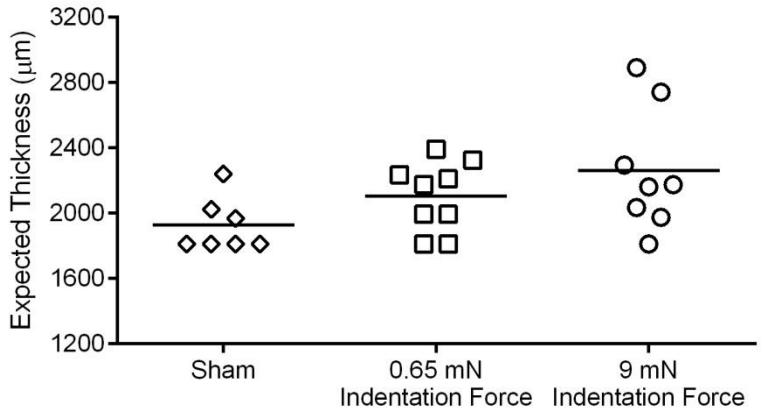

Figure S11 Caption: Distribution of expected corneal thicknesses between specimens of all experimental groups (p = 0.08).

Bibliography

Chernov, N., 2009. Circle Fit (Taubin method).

https://www.mathworks.com/matlabcentral/fileexchange/22678-circle-fit--taubin-method

(accessed 03/23/2015).